Rolling 2D Bioelectronic film into 1D: a Suturable Long-term Implantable Soft Microfiber

Ruijie Xie[1,2]†, Qianhengyuan Yu[1]†, Dong Li[3]†, Xu Han[2], Xiaolong Xu[2], Jianping Huang[1], Xiaomeng Zhou[1], Qiong Tian[1], Qingsong Li[1], Hanfei Li[1], Guanglin Li[1], Fei Han[1]*, Tiantian Xu[3]*, Zhiyuan Liu[1]*

Affiliations:

[1] CAS Key Laboratory of Human-Machine Intelligence-Synergy Systems, Shenzhen Institutes of Advanced Technology, Chinese Academy of Sciences (CAS), Shenzhen, 518055, China

[2]The Institute of Flexible Electronics (IFE, Future Technologies), Xiamen University, Xiamen 361005, Fujian, China

[3]The Guangdong Provincial Key Laboratory of Robotics and lntelligent System, Shenzhen Institute of Advanced Technology, Chinese Academy of Sciences, Shenzhen 518055 China

*Corresponding author. Email: zy.liu1@siat.ac.cn; tt.xu@siat.ac.cn; fei.han@siat.ac.cn.

† These authors contributed equally to this work.

Abstract: Long-term implantable intramuscular monitoring can efficiently evaluate the function of neuromuscular system. Film-shaped bioelectrodes require large implantation incisions inducing severe immune rejection. We report a soft and stretchable multifunctional microwire electrode array by rolling up a patterned sub-micro-thickness film. It possesses a stretchability of ~100% and can be sutured into muscle with the incision width of < 200 μm, allowing simultaneous acquisition of EMG and strain signals for at least 16 weeks in rats. The fibroblast encapsulation is negligible after 13 months implantation. Moreover, it can wander inside a brain with the assistance of magnetic force. The proposed strategy opens up the study of multi-channel and -function soft and stretchable wire-shaped sensors. It also provides a minimally invasive implantation platform for biomedical and healthcare applications.

One-Sentence Summary: A 60-channel EMG electrode and strain sensors were integrated into a 170 μm diameter stretchable wire sensor.

Neuromuscular system provides the basic kinetic energy for daily physiological activities of human body, such as the movement of the body's limbs[1,2], heart stripes[3,4], intestinal peristalsis[5,6], and so on. While working, it emits electrophysiological[7] and mechanical signals[8] that can be monitored by sensors, especially soft sensors with mechanical properties similar to human tissues and stretching with them.[9-12] By those signals, its functional state is evaluated and vital for extensive applications of human-machine interface and healthcare.[13-16]

These soft and stretchable sensors are mainly categorized into body surface sensors and implantable ones.[17-20] Soft sensors attached to the skin can only collect the average signal of the whole muscle bundles underneath, especially from the superficial muscles.[21-23] It is difficult for them to make a differentiation of those signals, whereas the implantable sensor allows accurate monitoring of deep muscles and their components: muscle motor units.[24-26] This implantable monitoring is desirable for precise understanding of muscles working process and significantly helpful for the control system in human-machine interface.[18] For example, Max Ortiz-Catalan et al. implanted electrodes in human body for up to 7 years to continuously collect myoelectric signals and control the prosthetic limb.[27] The rigid commercialized electrode was used with only four channels and implanted on the muscle dura rather than inside the muscle bundle, therefore few controlling freedoms achieved.

So, how to achieve the long-term monitoring inside the muscle bundle to enrich the signal collection? Firstly, the electrode needs to be put inside muscles with minimum surgery incision to lower or avoid the immune rejection effect.[28,29] Wire electrode could be the good candidate. It can be sutured into the muscle bundle with neglected injury to muscles. In comparison, thin film electrodes require complicated surgery process with skin and muscles severely damaged.[30] Secondly, it should be soft and stretchable just like the targeted muscle.[31] Thirdly, multi channels along the wire are desired to detect myoelectric signals along the muscle bundle. Therefore, a soft and stretchable wire with multi-channel stretchable electrodes along its axis would be one of the best candidates for long-term implantable monitoring.

For wire-like electrodes, the elongated thin film (hundreds micrometers in width, several micrometers in thickness or thinner, several centimeters in length) fabricated by photolithography is well developed to longitudinally fabricate multiple electrodes, while the substrate used was usually rigid and not stretchable.[32-35] Besides, depositing conductive film on stretchable wires through dip-coating method was proposed, and pre-stretching the wire prior to the deposition can further enhance the device's strechability.[36-38] It was also proposed to twist multiple fibers into a wire to achieve multifunctionality.[39] Moreover, thermal drawing process has been widely adopted to fabricate wire-shaped sensors. Also, it was relatively facile to fabricate multi channels/function sensors in the cross section of the wire, but not along the wire.[40] Therefore, we still need to find a facile strategy to fabricate a stretchable wire with multiple channels longitudinally distributed. It would be a big challenge, especially for a wire with hundreds of micrometers in diameter. It is tough to apply photolithography on one single microwire, to do the encapsulation for multiple channels and to integrate multiple functions along one single microwire.

In this article, we report a new strategy of rolling up patterned nano-thickness stretchable film into a microwire with up to 60-channel electrodes along one single microwire. During the rolling-up process, the electrodes are self-encapsulated. Inside the wire, the overlap of adjacent electrodes forms a capacitive stretchable strain sensor (Figure 1a). Therefore, it can detect bio-electrical and mechanical signals simultaneously. The microwire keeps conductive when stretched to around 100%. It can be sutured into the muscle bundle with an incision of less than 200 μm in width to continuously monitor both myoelectric signals and mechanical deformation of the muscle for at

least 16 weeks (Figure 1b). After up to 13-month implantation inside rats' muscle bundle, it is observed that the inflammation effect and the fibroblast encapsulation (with only ~ 23 μm in thickness) are much weaker than the control group with the rigid wire implanted. Our study provides the evidence that the soft and stretchable wire electrode has superior performance in long-term implantation in muscle bundle compared to the rigid one. It is also demonstrated that the soft microwire electrode array can "dive" and "wander" in the brain with the assistance of magnetic force. The proposed strategy opens up the study of multi-channel and -function soft and stretchable wire-shaped sensors, especially for that with function units longitudinally distributed. Following our strategy, more functional units could be rolled up into a wire. It also provides a minimally invasive implantation platform for biomedical and healthcare applications, enabling the biomedical studies and related applications with the requirement of long-term monitoring of physiological signals.

Fabrication of stretchable multifunctional wire sensor

The conductive pathway on the film electrode was fabricated by depositing Au on 400 nm thick SEBS film using a vacuum thermal evaporator. The pattern of the conductive path is designed as "C" shape and "L" shape. For the C-shaped pattern, when rolled up, two interconnected conductive points are exposed along the wire, one for the EMG electrode and the other for signal transmission. After two adjacent L-shaped patterns are rolled, one side of these two L-shaped patterns overlap to form a capacitor, and the other side of these two L-shaped patterns form two signal transmission points along the wire. To roll up the patterned film electrode, it was first lifted from the substrate and then rolled up to form a wire. Due to the interaction between film and substrate, a strain is induced on the film electrode (Figure S1a), which can also be confirmed from the SEM image of the fabricated wire electrode (Figure S1b). Thus, for the successful fabrication of the wire sensor, two factors have to be considered: on the one hand, the adsorption force between the substrate and the film electrode should be as low as possible to make the roll-up process feasible. Polytetrafluoroethylene was chosen as the substrate because of its excellent hydrophobicity, which made it have a lower force with SEBS.

On the other hand, good stretchability is necessary for successful roll-up of the film electrode. The stretchability of the conductive film was investigated by adjusting the thickness of the gold films and the width of the conductive pathway. As shown in Figure S2a, for a given width of the conductive path, the stretchability of the conductive film was initially increased and then decreased with increasing thickness of the gold film, reaching an optimum stretchability of 60% when 30 nm gold was deposited on SEBS film. Furthermore, the density of the wire electrode was determined by the width of the conductive path. It can be observed from Figure S2b that the stretchability of the electrode decreases as the conductive path narrows. When the width of the conductive path of the electrode is 200 μm, its stretchability is 30%. Using this parameter, a wire with a 60-channel electrode (Figure 1c) and a stretchability of 30% (Figure S3) was successfully obtained.

The diameter of the wire varies depending on the width of the film electrode. It can be observed that the center of the wire electrode with a diameter of 8 μm was disordered. (Figure 1d) As this disordered structure would affect the conductivity of the electrode, the diameter of the wire electrode should be larger than 8 μm. To improve the yield of the wire electrode, it is necessary to leave an empty space of 1 cm in front of the conductive path. (Figure S4) The minimum diameter of the wire is therefore 109 μm. When the film width exceeds 1 cm, the wire diameter increases by approximately 23.94 μm for each 1 cm increase in film electrode width. (Figure S5)

Performance stretchable multifunctional wire sensor

Typically, a 3 cm wide four-channel film electrode with two 'L' and two 'C' shaped channels was used to illustrate the performance of the wire electrode. The width of the channels and the space between them was 2 mm. (Figure S4b) The diameter of the fabricated wire was 170 μm. To transmit the information from the muscle, the wire sensor was connected to a printed circuit board (PCB) via anisotropic conductive films (ACF), then the PCB was connected to a rigid signal acquisition device via stainless steel wire by welding method. (Figure S6) As the muscle stretches during movement, good stretchability was necessary to ensure dynamic contact of the device with the muscle to improve signal quality, and also important to reduce immune rejection. Since the implanted part contains the wire sensor and its connector to the PCB, the sensing performance of the whole system is tested during stretching of the wire sensor with the connector. (Figure 2a) It can be seen from Figure S7 that the EMG electrode can maintain conductivity when the sensor is stretched to 60%. And the stretchability of the wire electrode increases to 94% after being stretched to 60% for 200 times, which is due to the formation of microcracks in the Au layer. (Figure 2b) The wire sensor was then stretched from 0% to 30% for 1000 cycles to test its stability. As shown in Figure 2c, the EMG electrode has a low resistance after the test. In addition, the capacitance formed by two adjacent channels will deform with the stretching of the wire sensor, which makes the wire can also act as a capacitive strain sensor to monitor the deformation induced by muscle stretching. (Figure 2d) The wire sensor showed a Gauge Factor of 0.96 (the theoretical maximum value is 1) and good linearity (R^2=0.998) within a strain interval of 40%. (Figure 2e) As the device is stretched, the SEBS between the two channels becomes thinner and when the device is stretched beyond 40%, the electrons pass through the SEBS between the channels reducing the device's capacitance, so the wire sensor's operating interval is 40%. Due to its high sensitivity, the 0.1% strain was detected by the wire sensor (Figure 2f), making it suitable for detecting the tiny deformation of the muscle during movement. Furthermore, since a large hysteresis curve would lead to irreversible sensing performance of the sensor under dynamic conditions, the wire sensor was stretched and then released to test its hysteresis curve. It can be seen in Figure 2g that there is no obvious hysteresis curve for the wire sensor. The sensor was then repeatedly stretched to 20% to test its stability. After stretching to 1000 cycles, the signal remained basically the same as in the initial state (Figure S8), indicating the good stability of the wire strain sensor. Since the impedance between the electrode and the tissue during movement determines the performance of the EMG electrode, the impedance of the wire electrode was also tested under stretching state. As shown in Figure 2h, after 30% stretch, the impedance of the device is increased when the frequency exceeds 1000 Hz, mainly due to the increase in electrode resistance. While it is almost unchanged when the frequency is below 1000 Hz, which provides the basis for stable EMG signal acquisition during muscle stretch.

Furthermore, the strategy proposed here was also applicable to other polymer substrates. For example, the multi-channel EMG and strain composite stretchable wire sensors were successfully fabricated by the rolling up of patterned ethylene-vinyl acetate copolymer-based film electrode and polydimethylsiloxane-based film electrode. (Figure S9) It should be noted that the good tear resistance was important to enhance the success of the wire devices, as the polymer films with low tear resistance were prone to tear and lead to the failure of the wire device fabrication.

For the implantable electronics, the interstitial fluid can penetrate the interface and cause failure of the ACF, breaking the circuit between the wire sensor and the PCB. Two waterproof layers of parafilm and 703 silicone were applied to improve the waterproofness of the interface. (Figure S6) The wire sensor with interface was then immersed in phosphate buffered saline at 37°C to simulate its working environment in vivo. It can be seen from Figure 2i that the impedance of

the EMG electrode showed negligible variation over 30 days, indicating that the interface designed here has the potential to work in the body.

Implantation of wire sensor in brain through magnetic field guidance

Another important factor affecting the degree of tissue damage caused by device implantation is the implantation method. Since needles can move in the presence of a magnetic field, it may be possible to achieve minimally invasive implantation of wire sensors connected to needle in deep tissue under magnetic field guidance. The feasibility of this approach is verified by implanting wire sensors in the brain. Using deep brain implantation electrodes to accurately monitor the brain's electrical activity is critical to both the treatment of brain disorders and the advancement of human-machine interfaces. Because the brain is enclosed within the skull, current implantation methods often require opening the skull, causing discomfort to patients and posing risks to their recovery. As shown in Figure 3a, the magnetic guidance method allows the wire electrode to be implanted through a 1 mm diameter skull opening. After electrode implantation, EEG signals were successfully monitored. (Figure 3b and Figure S10) For device implantation in the brain, damage to the blood-brain barrier is considered to be the initiation of the immune reaction. Therefore, reducing the damage to the blood vessels during device implantation can effectively prevent the degradation of electrode performance. A hydrogel-filled cerebrovascular scaffold was used to simulate brain tissue (Figure S11). As shown in Figure 3c and 3d, by controlling the position and rotation speed of an external rotating magnet, the position and orientation of the wire electrode could be effectively controlled, enabling precise three-dimensional movement of the wire electrode and allowing the electrode to avoid blood vessels and be successfully implanted in the brain model. Furthermore, to simulate how the wire electrode collects signals during movement, five hydrogels are arranged side-by-side, with each hydrogel applying a different simulated signal. (Figure 3e) When the wire device is passed through the different hydrogels sequentially under a magnetic field, different analogue signals can be detected at different locations. (Figure 3f) These results suggest that wire sensors can be guided by magnetic fields for minimally invasive implantation in the brain, and also provide a new minimally invasive implantation method for wire devices.

Long-term monitoring performance of wire sensor for muscle information

The wire can also be sutured into tissue like a surgical thread for minimally invasive implantation. As shown in Figure 4a and Figure S12, the wire was connected with a needle by surgical thread. After the needle inserted into the muscle, the wire device can be pulled into the muscle. Then an interface for transmitting signals to the signal acquisition device was placed on the head of the rat to avoid the damage of the interface by the rat. (Figure 4b) This strategy allows the EMG and strain signals to be monitored from the interface while the rat is moving freely. (Figure 4c) Before implanting the wire sensor, it is important to ensure its ability to simultaneously monitor multi-channel EMG signals. The EMG signal induced by stimulation of the sciatic nerve was then recorded by the wire electrode. It can be seen from Figure S13 that as the applied current increases, the amplitude of the EMG signals recorded by the wire sensor increases accordingly. The signals from the different channels show significant differences due to the different distance of each channel from the stimulation site, indicating that the channels are not influenced by each other when monitoring the EMG signals. Furthermore, monitoring induced EMG is a standard method for clinical assessment of nerve damage. As shown in Figure S14, the nerve between the muscle and the stimulation site was damaged by clamping it with different forces, and for a stimulation current of 36 μA, the amplitude of the EMG signals decreases with increasing degree of damage. When the nerve was severely damaged, no EMG signal was detected even at a

stimulation current of 200 μA, suggesting the good ability of the wire sensor to assess nerve damage.

The wire electrode system was then implanted into the rat to monitor the information from the muscle. When both channels were sutured into the tibialis anterior muscle, the EMG signals from both channels showed a similar profile. (Figure S15) Moreover, every movement of the human body involves at least two muscles, it is essential for the EMG prosthetic control to monitor the EMG signals from multiple muscles simultaneously. However, implanting an electrode in each muscle will cause severe tissue damage and increase the risk of infection. Since the manufactured wire sensor has multiple channels, it is possible to acquire EMG signals from several muscles with one wire sensor. In the rat, the tibialis anterior and the gastrocnemius are the two most important muscles for the movement of the hind legs. A wire sensor was then sutured into the tibialis anterior and gastrocnemius muscles simultaneously, leaving one channel in each muscle. As can be seen from Figure 4d, two different EMG signals were recorded from the two muscles, suggesting the ability of the wire sensor to obtain EMG information from different muscles simultaneously. In addition, as the wire sensor stretched with the muscle during the rat's movement, the strain information in the muscle would be reflected in the wire sensor. As shown in Figure 4e, when the hind leg of the rat was stretched, the strain induced in the muscle was successfully detected. Thus, the wire sensor reported here can be implanted in animals by minimally invasive implantation to monitor the EMG and strain signals of muscles.

For the application of the wire sensor in prosthetic control, it should show long-term stability after implantation. The wire sensor was implanted in the anterior tibial muscle and the EMG signal was recorded every week to assess its long-term stability. For comparison, a four-channel film electrode with a thickness of 100 μm and a stainless-steel electrode with a diameter of 170 μm were also implanted in the tibial anterior muscle. It can be observed from Figure S16 that the spread of the film electrode in the muscle requires a large wound, which will make the film electrode cannot contact the muscle during the rat's movement. For the stainless-steel electrode, it can be implanted in the muscle by the same method with the wire sensor, while its high Young's modulus will lead to its relative slipping with the muscle. Due to the stretchability of the composite wire sensor, when sutured into the muscle, it will continue to adhere to the muscle during stretching of the muscle, resulting in a higher signal-to-noise ratio than the film electrode and the stainless-steel electrode. After 16 weeks, the wire sensor still showed a significant advantage in signal-to-noise ratio over the other sensors (Figure 4f). After these sensors had been implanted in the muscle for 1 year, tissue staining was performed to evaluate the influence of the sensor on the muscle. As shown in Figure 4g, the hematoxylin-eosin staining result indicated that the thickness of fibrotic tissue around the wire sensor was less than 23 μm and no significant changes in the structure of the muscle bundle were observed, while that around the stainless-steel electrode exceeded 481 μm, which can also explain the higher signal-to-noise ratio of the composite wire sensor. Furthermore, it can be observed from the result of immunofluorescence staining (Figure 4i) and TDT-mediated dTUP nick end labelling (Figure 4j) that the fluorescence intensity around the wire sensor shows an undetectable change compared to the normal tissue, indicating low connective tissue growth factor concentration (positively correlated with the formation of fibrotic tissue) and low apoptosis level. However, for the stainless-steel electrode, the fluorescence intensity around it has a significant increase compared to the normal tissue. (Figure 4k and 4l) Thus, it can be concluded that the fabricated wire sensor has good biocompatibility and stable performance during long-term implantation, which can be attributed to its smaller implant wounds and stretchability.

Conclusion

In summary, a multi-channel EMG and strain composite stretchable wire sensor was fabricated by rolling a patterned film stretchable electrode up. By adjusting the width of the conductive pathway, it is possible to integrate 60 channels of EMG electrodes on a wire with a diameter of 170 μm. It can act as a surgical suture into multiple muscles to monitor the EMG signals of multiple muscles simultaneously, with an implantation incision of no more than 200 μm. The high sensitivity of its capacitive strain sensor section allows it to detect 0.1% deformation, enabling it to measure muscle strain as the rat leg is stretched. It can function normally in vivo for at least 16 weeks. Due to its small implantation incision and stretchability, it has almost no effect on the surrounding muscles after implantation for one year. In addition, by controlling the needle with a magnet, minimally invasive implantation of wire devices in the deep tissue can also be achieved. The proposed strategy provides a platform for the preparation and minimally invasive implantation of multifunctional wire sensors.

References and Notes

1 Kuiken, T. A. *et al.* Targeted Muscle Reinnervation for Real-time Myoelectric Control of Multifunction Artificial Arms. *JAMA, J. Am. Med. Assoc.* **301**, 619-628 (2009). 10.1001/jama.2009.116.

2 Salminger, S. *et al.* Long-term implant of intramuscular sensors and nerve transfers for wireless control of robotic arms in above-elbow amputees. *Sci. Robot.* **4**, eaaw6306 (2019). 10.1126/scirobotics.aaw6306.

3 Liu, J. *et al.* Intrinsically stretchable electrode array enabled in vivo electrophysiological mapping of atrial fibrillation at cellular resolution. *Proc. Natl. Acad. Sci. U. S. A.* **117**, 14769-14778 (2020). 10.1073/pnas.2000207117.

4 Fang, H. *et al.* Capacitively coupled arrays of multiplexed flexible silicon transistors for long-term cardiac electrophysiology. *Nat. Biomed. Eng.* **1**, 0038 (2017). 10.1038/s41551-017-0038.

5 Spencer, N. J. & Hu, H. Z. Enteric nervous system: sensory transduction, neural circuits and gastrointestinal motility. *Nat. Rev. Gastroenterol. Hepatol.* **17**, 338-351 (2020). 10.1038/s41575-020-0271-2.

6 Yao, G. *et al.* Effective weight control via an implanted self-powered vagus nerve stimulation device. *Nat. Commun.* **9**, 5349 (2018). 10.1038/s41467-018-07764-z.

7 Tian, Q. *et al.* Hairy Skin-adaptive Viscoelastic Dry Electrodes for Long-term Electrophysiological Monitoring. *Adv. Mater.* **35**, 2211236 (2023). 10.1002/adma.202211236.

8 Lee, J. *et al.* Stretchable and suturable fibre sensors for wireless monitoring of connective tissue strain. *Nat. Electron.* **4**, 291-301 (2021). 10.1038/s41928-021-00557-1.

9 Tian, L. *et al.* Large-area MRI-compatible epidermal electronic interfaces for prosthetic control and cognitive monitoring. *Nat. Biomed. Eng.* **3**, 194-205 (2019). 10.1038/s41551-019-0347-x.

10 Wang, W. *et al.* Neuromorphic sensorimotor loop embodied by monolithically integrated, low-voltage, soft e-skin. *Science* **380**, 735-742 (2023). 10.1126/science.ade0086.

11 Abramson, A. *et al.* A flexible electronic strain sensor for the real-time monitoring of tumor regression. *Sci. Adv.* **8**, eabn6550 (2022). 10.1126/sciadv.abn6550.

12 Cui, Z. *et al.* Haptically Quantifying Young's Modulus of Soft Materials Using a Self-Locked Stretchable Strain Sensor. *Adv. Mater.* **34**, 2104078 (2022). 10.1002/adma.202104078.

13 Zarei, M., Lee, G., Lee, S. G. & Cho, K. Advances in biodegradable electronic skin: Material progress and recent applications in sensing, robotics, and human–machine interfaces. *Adv. Mater.* **35**, 2203193 (2023). 10.1002/adma.202203193.

14 Jiang, Y. *et al.* A universal interface for plug-and-play assembly of stretchable devices. *Nature* **614**, 456-462 (2023). 10.1038/s41586-022-05579-z.

15 Laffranchi, M. *et al.* The Hannes hand prosthesis replicates the key biological properties of the human hand. *Sci. Robot.* **5**, eabb0467 (2020). 10.1126/scirobotics.abb0467.

16 Heng, W. Z., Solomon, S. & Gao, W. Flexible Electronics and Devices as Human-Machine Interfaces for Medical Robotics. *Adv. Mater.* **34**, 2107902 (2022). 10.1002/adma.202107902.

17 Wang, X., Liu, Y., Cheng, H. & Ouyang, X. Surface Wettability for Skin-Interfaced Sensors and Devices. *Adv. Funct. Mater.* **32**, 2200260 (2022). 10.1002/adfm.202200260.

18 Heng, W., Solomon, S. & Gao, W. Flexible electronics and devices as human–machine interfaces for medical robotics. *Adv. Mater.* **34**, 2107902 (2022). 10.1002/adma.202107902.

19 Li, J. *et al.* A tissue-like neurotransmitter sensor for the brain and gut. *Nature* **606**, 94-101 (2022). 10.1038/s41586-022-04615-2.

20 Lee, Y. *et al.* A low-power stretchable neuromorphic nerve with proprioceptive feedback. *Nat. Biomed. Eng.* **7**, 511-519 (2023). 10.1038/s41551-022-00918-x.

21 Serrano, R. R. M. *et al.* High Density Body Surface Potential Mapping with Conducting Polymer-Eutectogel Electrode Arrays for ECG imaging. *Adv. Sci.*, 2301176 (2023). 10.1002/advs.202301176haode

22 Tringides, C. M. *et al.* Viscoelastic surface electrode arrays to interface with viscoelastic tissues. *Nat. Nanotechnol.* **16**, 1019-1029 (2021). 10.1038/s41565-021-00926-z.

23 Xie, R. J. *et al.* Strenuous exercise-tolerance stretchable dry electrodes for continuous multi-channel electrophysiological monitoring. *npj Flexible Electron.* **6**, 75 (2022). 10.1038/s41528-022-00209-0.

24 Sang, M., Kim, K., Shin, J. & Yu, K. J. Ultra-Thin Flexible Encapsulating Materials for Soft Bio-Integrated Electronics. *Adv. Sci.* **9**, 2202980 (2022). 10.1002/advs.202202980.

25 Boutry, C. M. *et al.* Biodegradable and flexible arterial-pulse sensor for the wireless monitoring of blood flow. *Nat. Biomed. Eng.* **3**, 47-57 (2019). 10.1038/s41551-018-0336-5.

26 Shen, K., Chen, O., Edmunds, J. L., Piech, D. K. & Maharbiz, M. M. Translational opportunities and challenges of invasive electrodes for neural interfaces. *Nat. Biomed. Eng.* **7**, 424-442 (2023). 10.1038/s41551-023-01021-5.

27 Ortiz-Catalan, M., Mastinu, E., Sassu, P., Aszmann, O. & Brånemark, R. Self-contained neuromusculoskeletal arm prostheses. *N. Engl. J. Med.* **382**, 1732-1738 (2020). 10.1056/NEJMoa1917537.

28 Zhou, G. & Groth, T. Host responses to biomaterials and anti-inflammatory design—a brief review. *Macromol. Biosci.* **18**, 1800112 (2018). 10.1002/mabi.201800112.

29 Feiner, R. & Dvir, T. Tissue-electronics interfaces: from implantable devices to engineered tissues. *Nat. Rev. Mater.* **3**, 17076 (2018). 10.1038/natrevmats.2017.76.

30 Uguz, I. & Shepard, K. L. Spatially controlled, bipolar, cortical stimulation with high-capacitance, mechanically flexible subdural surface microelectrode arrays. *Sci. Adv.* **8**, eabq6354 (2022). 10.5281/zenodo.6972414.

31 Jiang, Z. *et al.* A 1.3-micrometre-thick elastic conductor for seamless on-skin and implantable sensors. *Nat. Electron.* **5**, 784-793 (2022). 10.1038/s41928-022-00868-x.

32 Hong, G. S. & Lieber, C. M. Novel electrode technologies for neural recordings. *Nat. Rev. Neurosci.* **20**, 330-345 (2019). 10.1038/s41583-019-0140-6.

33 Musk, E. An Integrated Brain-Machine Interface Platform With Thousands of Channels. *J. Med. Internet Res.* **21**, e16194 (2019). 10.2196/16194.

34 Guan, S. *et al.* Elastocapillary self-assembled neurotassels for stable neural activity recordings. *Sci. Adv.* **5**, eaav2842 (2019). 10.1126/sciadv.aav2842.

35 Luan, L. *et al.* Ultraflexible nanoelectronic probes form reliable, glial scar-free neural integration. *Sci. Adv.* **3**, e1601966 (2017). 10.1126/sciadv.1601966.

36 Lee, G. H. *et al.* Conductance stable and mechanically durable bi-layer EGaIn composite-coated stretchable fiber for 1D bioelectronics. *Nat. Commun.* **14** (2023). 10.1038/s41467-023-39928-x.

37 Shi, X. *et al.* Large-area display textiles integrated with functional systems. *Nature* **591**, 240-245 (2021). 10.1038/s41586-021-03295-8.

38 Chen, C. R. *et al.* Functional Fiber Materials to Smart Fiber Devices. *Chem. Rev.* **123**, 613-662 (2023). 10.1021/acs.chemrev.2c00192.

39 Wang, L. Y. *et al.* Functionalized helical fibre bundles of carbon nanotubes as electrochemical sensors for long-term in vivo monitoring of multiple disease biomarkers. *Nat. Biomed. Eng.* **4**, 159-171 (2020). 10.1038/s41551-019-0462-8.

40 Park, S., Loke, G., Fink, Y. & Anikeeva, P. Flexible fiber-based optoelectronics for neural interfaces. *Chem. Soc. Rev.* **48**, 1826-1852 (2019). 10.1039/c8cs00710a.

Acknowledgments: During the course of this work, we discovered similar approach on using rolling to prepare soft bioelectronic fiber is being pursued by Zhenan Bao Group in Stanford University. We jointly decided to post our work simultaneously in BioRxiv. The work from Bao Group is entitled “Spiral NeuroStrings: high-density multimodal soft bioelectronic fibers” by M. Khatib, E.T. Zhao, S. Wei, J. Dunn and Z, Bao et al.

We thank the Institutional Animal Care and Use Committee (IACUC) of Shenzhen Institute of Advanced Technology Chinese Academy of Sciences. All the animal experiments performed in

this research were approved by the IACUC under the protocols of SIAT-IACUC-210316-JCS-XRJ-A1740-01.

Funding: this work was supported by National Natural Science Foundation of China (62101545), National Key R&D Program of China (2021YFF0501601, 2021YFF0501602), Shenzhen Science and Technology Program (KQTD20210811090217009), National Natural Science Foundation of China (62101544, 62201558, and 62201559), and Guangdong Basic and Applied Basic Research Foundation (2020A1515110205), the Fundamental Research Funds for the Central Universities (20720230041). This work was partially supported by Shenzhen-Hong Kong Institute of Brain Science (NSY889021054) and the Science and Technology Program of Guangdong Province（2022A0505090007).

Author contributions: R. Xie conceived of this research, performed the experiments, and wrote the manuscript. Q. Yu performed the animal experiments and the ex vivo and in vivo EMG measurements, and J. Huang helped. D. Li and F. Han performed the implantation of the wire sensor under magnetic force and the EEG measurements. X. Han and X. Xu helped to draw illustrations. X. Zhou provided the test equipment. Q. Tian, Q. Li, and H. Fei participated in the discussions. G. Li supervised the project. T. Xu and Z. Liu supervised the project and revised the manuscript.

Competing interests: Authors declare that they have no competing interests.

Data and materials availability: All data are available in the main text or the supplementary materials.”

Supplementary Materials

Materials and Methods

Figs. S1 to S16

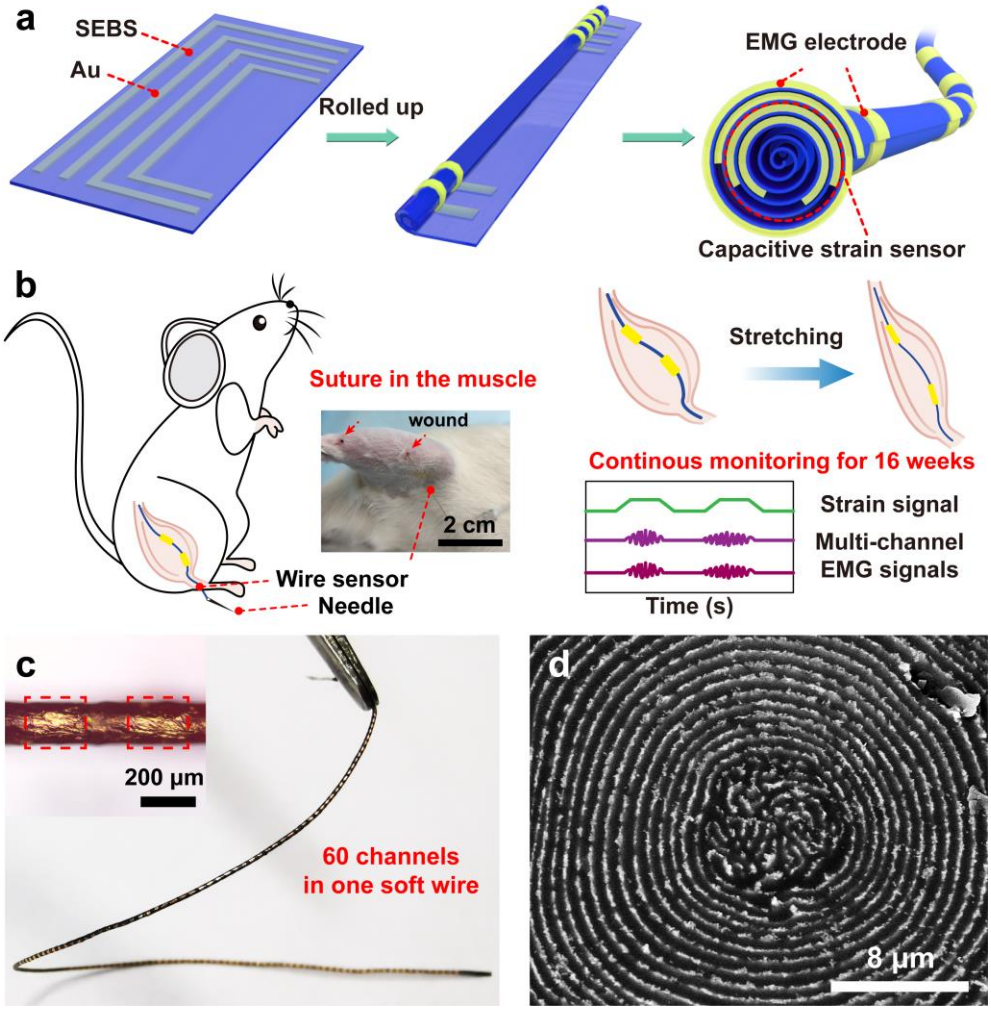

Fig. 1. Preparation strategy and advantages of wire sensor. a) Schematic diagram of the multifunctional wire the preparation process. b) Wire devices are sutured into rat muscle with a

puncture needle and monitoring multichannel EMG and strain signals for 16 weeks. c) A wire with 60-channel EMG electrode. d) SEM image of the cross section of the wire sensor.

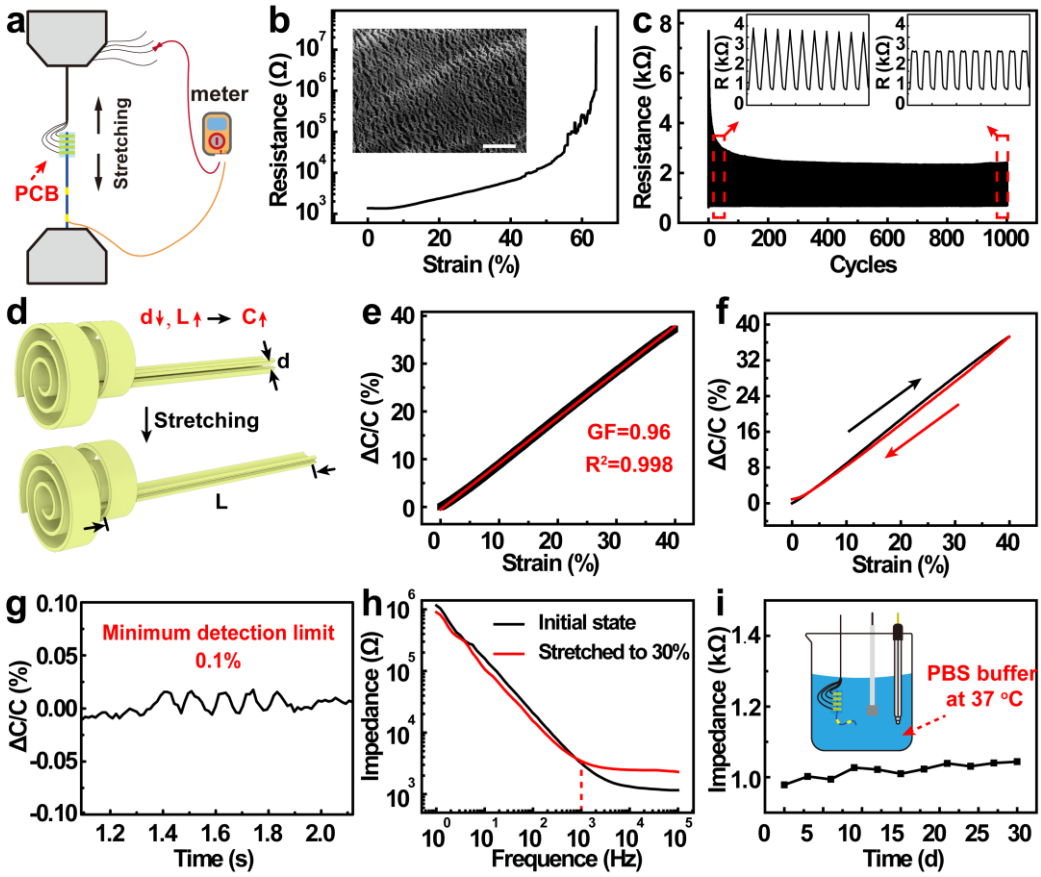

Fig.2. Performance of the wire sensor system. a) Illustration of the stretchability test for wire sensor systems. b) Stretchability of the wire sensor system, the image inside is the SEM image of the wire sensor in the stretched state. c) Durability of the wire sensor system after being stretched to 30% for 1000 cycles. d) Schematic illustration of the structural changes of the capacitor inside the wire during stretching e) Change in the relative change of capacitance under various strains; GF was obtained by linear fitting. f) Hysteresis curve for wire devices. g) Minimum detection limit

of the wire when used as capacitive stain sensor. h) Change in impedance of the wire electrode when stretched to 30%. i) Waterproofing tests for the wire sensor system.

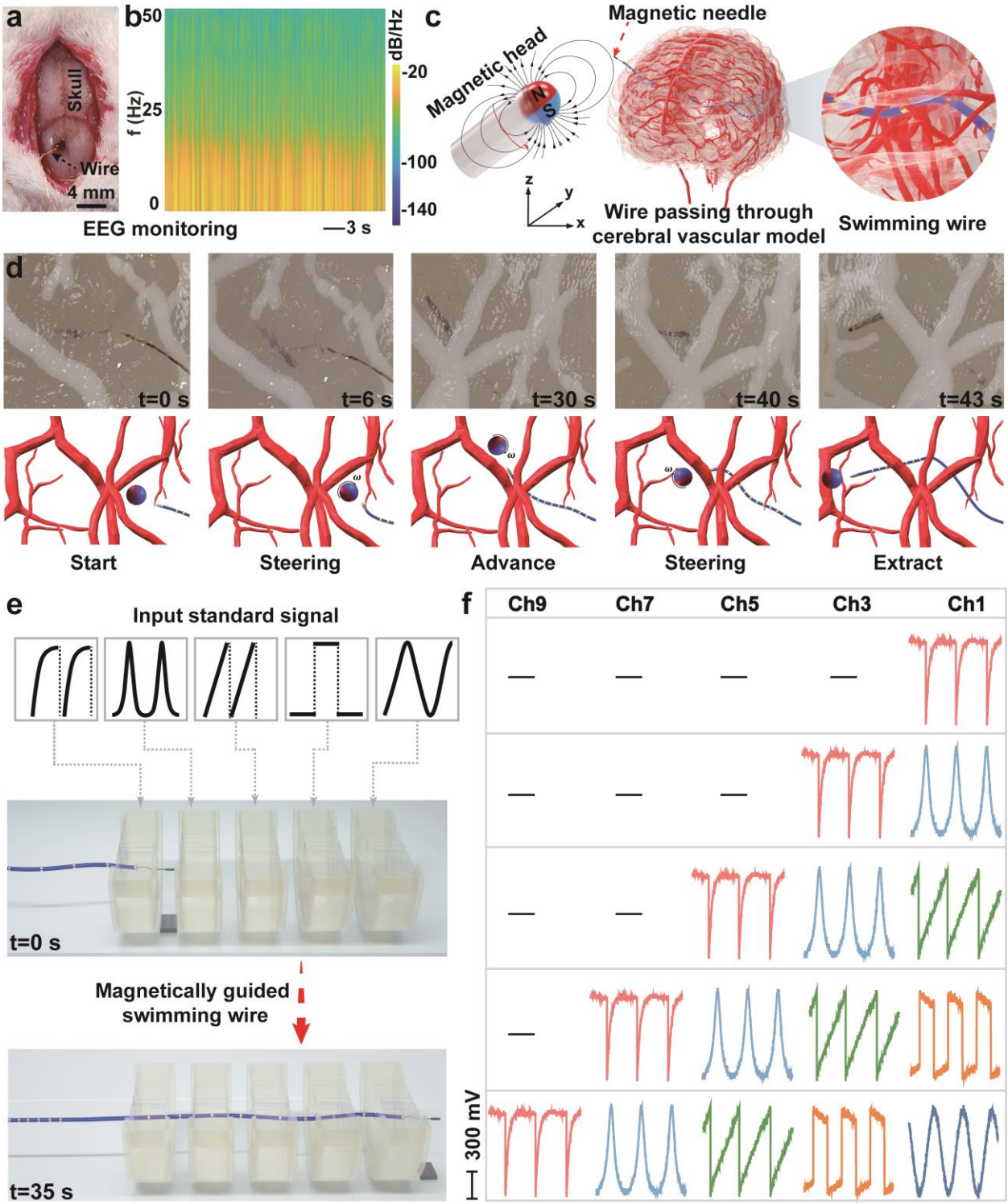

Fig. 3. Implantation of wire sensor under magnetic field. a) Implantation of wire electrodes into the rat brain through a small aperture. b) Continuous monitoring of electroencephalogram (EEG) frequency spectrums within 10 min through the wire electrode. c) Schematic illustration of

swimming wire in 3D printed cerebral vascular model guided by rotating magnetic head. d) The images and schematic diagrams of controllable swimming in agar-infused cerebral vascular model of wire electrode in 43 seconds. e) Schematics of swimming wire passing through five simulated neural units in sequence driven by external magnetic force. f) Recorded analog signals by swimming wire from five channels (Electrode 1 (Ch1), Electrode 3 (Ch3), Electrode 5 (Ch5), Electrode 7 (Ch7), Electrode 9 (Ch9)) in the process illustrated in Figure 3e.

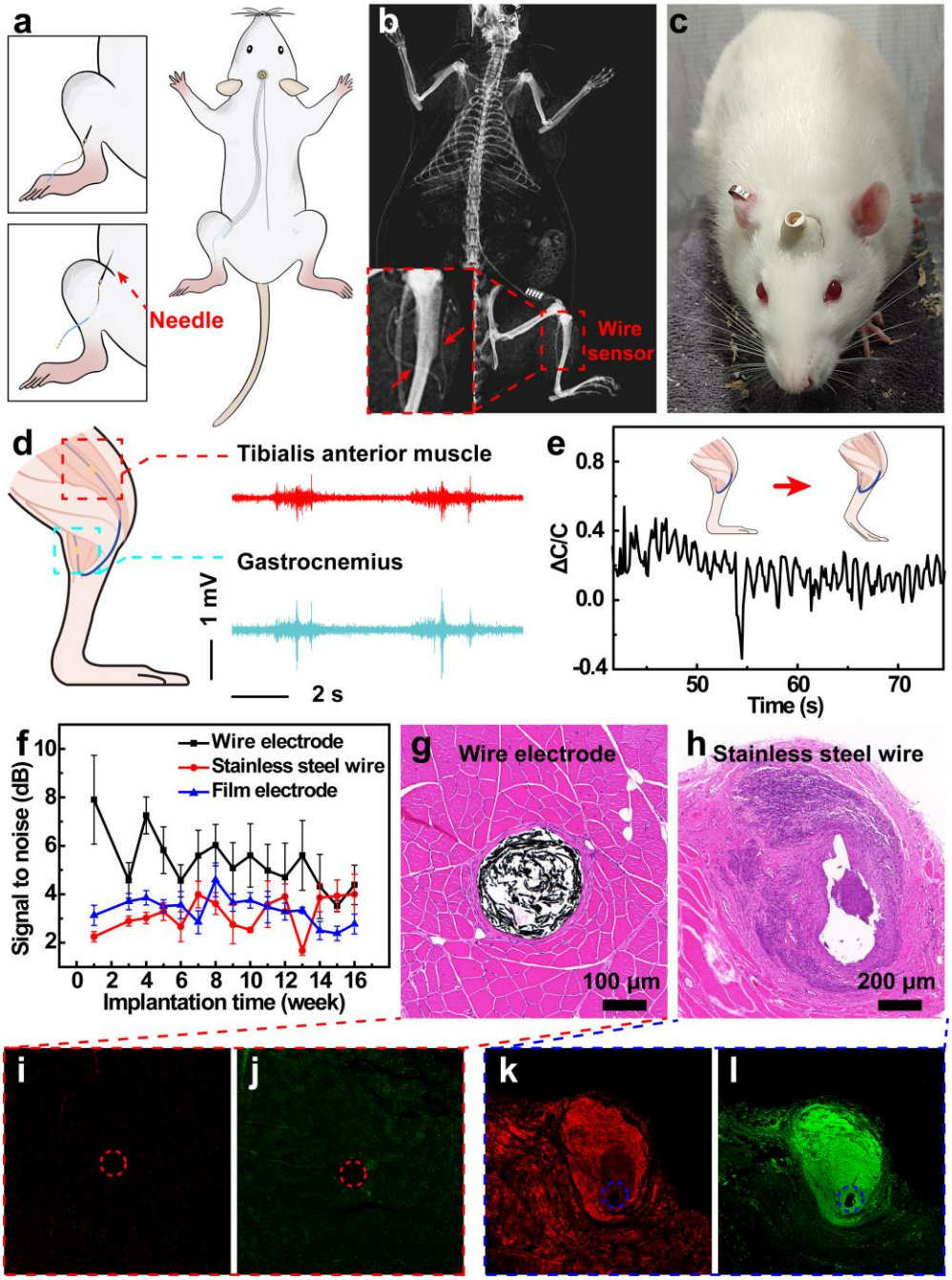

Fig. 4. Long-term monitoring performance of wire sensor for muscle information. a) Illustration of the wire sensor system implantation process. b) X-ray image of rat after implantation of a wire sensor system. c) Free movement of rat after wire sensor system implantation. d) Simultaneous acquisition of EMG signals from two muscles using the wire sensor system. e)

Muscle strain monitoring using a wire sensor system when stretching the rat's leg. f) Comparison of signal-to-noise ratio of wire sensors, stainless steel wire sensors and thin film sensors over 16 weeks after implantation. g-h) Hematoxylin-eosin staining results of tissue around stretchable wire sensor (g) and stainless-steel wire sensors (h), respectively. i-j) Immunofluorescence staining result (i) and TDT-mediated dTUP Nick-End Labeling result (j) of tissue around the stretchable wire sensor, respectively. k-l) Immunofluorescence staining result (k) and TDT-mediated dTUP Nick-End Labeling result (l) of tissue around the stainless-steel wire sensors, respectively.